# Near-optimal Order-reduced Control on Electric Vehicle for Both Comfortableness and Energy Consumption

Chien-Chin Chiu, Nan-Chyuan Tsai*, and Chun-Chi Lin

***Abstract*—**This work is aimed to investigate the regulation problem for thermal comfortableness and propose control strategies for cabin environment of electric vehicles (EVs) by constructing a reduced-scale air-conditioning (A/C) system which mainly consists of two modules: environmental control box (ECB) and air-handling unit (AHU). Temperature and humidity in the ECB can be regulated by AHU *via* cooling, heating, mixing air streams and adjusting speed of fans. To synthesize the near-optimal controllers, the mathematical model for the system thermodynamics is developed by employing the equivalent lumped heat capacity approach, energy/mass conservation principle and the heat transfer theories. In addition, from the clustering pattern of system eigenvalues, the thermodynamics of the interested system can evidently be characterized by two-time-scale property. That is, the studied system can be decoupled into two subsystems, slow mode and fast mode, by singular perturbation technique. As to the optimal control strategies for EVs, by taking thermal comfortableness, humidity and energy consumption all into account, a series of optimal controllers are synthesized on the base of the order-reduced thermodynamic model. The feedback control loop for the experimental test rig is examined and realized by the aid of the control system development kit dSPACE DS1104 and the commercial software MATLAB/Simulink. To sum up, the intensive computer simulations and experimental results verify that the performance of the near-optimal reduced control law is almost as superior as that of standard Linear Quadratic Regulator (LQR).

***Keywords*—**Singular Perturbation Technique, Near-Optimal Control, Thermal Comfort, Air-Conditioning System.

## I. Introduction

DUE to global warming and rapid decay of fossil energy reserve, recently hybrid electric vehicles (HEV) and electric vehicles (EV) have become new targets for the vehicle market. Among them, EV is specifically emphasized, owing to its property of zero emission. The air cooling mode of air-conditioning system for gasoline vehicle is realized by the compressor driven by engine, but in EV it is by motor (or called electric air-conditioning). On the other hand, the heating mode of air-conditioning system for gasoline vehicle is to employ the exhaust heat out of engine, but in EV it is driven by electric heater. For EV, the electric heater definitely consumes significantly partial battery energy. The evolution for EV is somehow deterred due to the problem of short mileage. As to the shortcoming of limited mileage, the electric energy provided by battery is consumed by air-conditioning system up to 30% [1]. Hence how to reduce energy loss for air-conditioning system in EV becomes a significant research target nowadays.

In order to analyze and improve the dynamic behavior of the air-conditioning system, at first it is necessary to establish the dynamic models of the air-conditioned space (ACS) and air-handling unit (AHU). Modeling techniques on air conditioning system can be divided into two categories. One is based on thermodynamic/heat transfer theory [2]-[6], while the other is based on experimental measurement data and system identification such as black-box method [7] and grey-box modeling technique [8].

For controller design, energy consumption is beyond the primary concern by these researches. Instead, the propose of this work is to employ an appropriate control policy particularly for the EV air-conditioning system such that the comfortableness for passengers, least energy consumption and electric power efficiency can be all taken into account together. To maintain the comfortableness of cabin environment, it is necessary to regulate not only interior temperature but also humidity. In order to reduce the energy consumption for general air conditioning process, a few optimal control strategies were reported [9]-[13]. Nevertheless, the dynamics of air conditioning system for EVs is pretty complicated, high-order and highly nonlinear. The singular perturbation theory is usually employed to deal with the plant with the presence of parasitic parameters. By singular perturbation technique, the plant can be split into two lower-order subsystems in two time scales. For controller synthesis, by singular perturbation method, the control laws can be developed for slow-mode subsystem and fast-mode subsystem separately. Therefore, the resulted composite control can be obtained by summation of the outputs of these two controllers [14]-[15].

In this paper, a scale-down experimental test rig of air

Chien-Chin Chiu, was with the Department of Mechanical Engineering, National Cheng Kung University, Tainan 70101, Taiwan. He is now with Hermes-Epitek, Hsinchu 300, Taiwan (e-mail: Jianchin721215@gmail.com).

*Nan-Chyuan Tsai, is with the Department of Mechanical Engineering, National Cheng Kung University, Tainan 70101, Taiwan (corresponding author to provide phone: +886-6-2757575 Ext. 62137; fax: +886-6-2369567; e-mail: nortren@mail.ncku.edu.tw).

Chun-Chi Lin, is with the Department of Mechanical Engineering, National Cheng Kung University, Tainan 70101, Taiwan (e-mail: n18991380@mail.ncku.edu.tw).

conditioning system to imitate the temperature/humidity of cabin in electric vehicle is constructed. After thermodynamic model linearization of system by taking Taylor's Expansion around the operational point, the thermodynamic models of the full system are derived and decoupled into two subsystems, "Slow Mode" and "Fast Mode", based on the singular perturbation technique. By considering the comfortableness for passengers, least energy consumption and electric power efficiency, a series of optimal controllers, namely near-optimal regulator, near-optimal reduced control and corrected linear quadratic regulator [16], are proposed for the EV air-conditioning system. In addition, the standard LQR plays the role of benchmark and is to be compared with the preliminarily proposed controllers. By computer simulation results, the efficacy of various optimal controllers proposed by this paper is all acceptable, with respect to the benchmark by LQR. The near-optimal reduced control strategy is the simplest and carries the least computation load so that it is chosen for the efficacy examination by experiments. The experimental results show that under near-optimal reduced control strategy, the preset temperature and humidity for cabin can be achieved and then retained not only at summer mode but also at winter mode.

## II. Thermodynamic Model of HVAC

### A. Configuration of HVAC Module

The HVAC module, shown in Fig. 1, mainly consists of two major portions. One is the cabin, referred to "Environmental Control Box (ECB)" in the experimental setup. The other is "Air-Handling Unit (AHU)" which can actively adjust the temperature and humidity of ECB. These two sub-systems are to be analyzed and discussed respectively in the following sections.

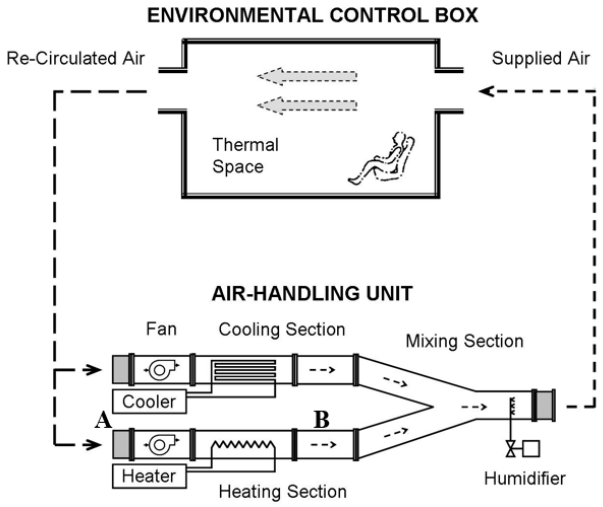


Fig. 1 Schematic of Environmental Control for Electric Vehicles

### B. Thermodynamic Model of Cabin

The cabin is mainly constituted by two physical elements: cabin wall and the air in cabin. The governing equations of energy conservation for the air in cabin and mass conservation, due to water vaporization, can be described respectively as follows[17]-[19]:

$$d\theta_{IN}/dt = (\tilde{f}_c + \tilde{f}_h)(\theta_S - \theta_{IN})/V_{IN} + h_g\Omega_p(\tilde{f}_c + \tilde{f}_h)[(Y_S - \beta_\theta\theta_S - \beta_c) - (Y_{IN} - \beta_\theta\theta_{IN} - \beta_c)]/\beta_p c_p V_{IN} + A_W^{IN}[\hat{h}_n + \hat{h}_f(\tilde{f}_c + \tilde{f}_h)^{2/3}/S_{IN}{}^{2/3}](\theta_W - \theta_{IN})/\rho_a c_p V_{IN} \quad (1)$$

$$d\theta_W/dt = A_W^O(\hat{h}_n + \hat{h}_f\gamma_O{}^{2/3})\{[\theta_O + \alpha I_t/(\hat{h}_n + \hat{h}_f\gamma_O{}^{2/3})] - \theta_W\}/C_W + A_W^{IN}\{\hat{h}_n + \hat{h}_f[(\tilde{f}_c + \tilde{f}_h)/S_{IN}]^{2/3}\}(\theta_{IN} - \theta_W)/C_W \quad (2)$$

where $A_W^{SH}$ is the effective surface area for the solar heat radiation applied upon the surface of cabin, SHGF the corresponding Solar Heat Gain Factor, SHGC the Solar Heat Gain Coefficient, $\rho_a$ the air density in cabin, $c_p$ the specific heat constant, $V_{IN}$ the volume of the air in cabin, $\Omega_p$ proportional coefficient, $\theta_{IN}$ the temperature in cabin, $\theta_S$ the temperature of AHU and $Q_{load}$ the heat load which causes the temperature of the cabin increased. $A_W^{IN}$ is the interior surface area of the cabin wall, $\theta_W$ the temperature of the cabin wall, $\hat{h}_n$ the heat transfer coefficient of natural convection, $\hat{h}_f$ the heat transfer coefficient of forced convection and $h_g$ the enthalpy of saturated vaporization. $\tilde{f}_h$ is the volume flow rate of air inside the heating section, $\tilde{f}_c$ the volume flow rate of air inside the cooling section, $A_W^O$ the exterior surface area of the cabin wall, $\alpha$ the absorptance of solar radiation, $I_t$ the irradiation of the exterior surface of cabin wall and $\gamma_O$ the wind speed of ambient environment. $\beta_\theta$, $\beta_p$ and $\beta_c$ are the corresponding coefficients of thermal sensation scale defined by ASHRAE (American Society of Heating, Refrigerating and Air-Conditioning Engineers) [19]. $Y_{IN}$ is the thermal sensation scale for the air in cabin and $Y_S$ the thermal sensation scale for the supplied air by AHU [19].

### C. Thermodynamic Model of Air-Handling Unit (AHU)

The AHU module, shown in Fig. 1, is mainly constituted by the air cooling/heating section, the mixing section and the humidifying section. The equation of energy conservation by the heater can be described as follows:

$$d\theta_H/dt = \tilde{f}_h(\theta_{IN} - \theta_H)/V_{HT} + A_{HT}[\hat{h}_n + \hat{h}_f(\tilde{f}_h/S_h)^{2/3}] \times[\theta_{HT} - (\theta_{IN} + \theta_H)/2]/\rho_a c_p V_{HT} \quad (3)$$

$$d\theta_{HT}/dt = A_{HT}[\hat{h}_n + \hat{h}_f(\tilde{f}_h/S_h)^{2/3}][(\theta_{IN} + \theta_H)/2 - \theta_{HT}]/C_{HT} + P_{HT}/C_{HT} \quad (4)$$

where $C_{HT}$ is the heat capacitance of the heater, $\theta_{HT}$ the temperature of the facial surface of the heater and $P_{HT}$ the supplied electric power by electric heater.

Based on the experimental setup shown in Fig. 1, the equations of thermodynamics and absolute humidity inside the

humidifying section can be expressed respectively as follows:

$$\begin{aligned} d\theta_S/dt = {} & \tilde{f}_{mix}[(\tilde{f}_c\theta_C + \tilde{f}_h\theta_H)/(\tilde{f}_c + \tilde{f}_h) - \theta_S]/V_{HF} \\ & + h_g\Omega_p\tilde{f}_{mix}[\tilde{f}_c p_C/(\tilde{f}_c + \tilde{f}_h) \\ & + \tilde{f}_h(Y_{IN} - \beta_\theta\theta_{IN} - \beta_c)/(\tilde{f}_c + \tilde{f}_h)\beta_p \\ & - (Y_S - \beta_\theta\theta_S - \beta_c)/\beta_p]/c_pV_{HF} \end{aligned} \quad (5)$$

where $\tilde{f}_{mix} = \tilde{f}_c + \tilde{f}_h$

$\tilde{f}_{mix}$ is the volume flow rate of mixed air composed by the cold air component, $\tilde{f}_c$, and the hot air component, $\tilde{f}_h$. $V_{HF}$ is the total volume of humidifying section.

### D. Comfort Temperature and Humidity

The two key factors on thermal comfortableness perceived by driver and guests in the car are: (i) air temperature (or called dry-bulb temperature) and (ii) relative humidity of air. The corresponding linear regression equation of thermal comfortableness can be expressed by [19]-[20]：

$$Y(\theta, p_v) = \beta_\theta\theta + \beta_p p_v + \beta_c \quad (6)$$

where $Y(\theta, p_v)$ is the so called "thermal sensation scale", $\theta$ the dry-bulb temperature, and $p_v$ the partial pressure of water vaporization. The physical value of $Y(\theta, p_v)$ indicates the degree of thermal sensation by human. The typical values are shown in Table I.

TABLE I
THERMAL SENSATION SCALE BY ASHRAE

| Value | Thermal Sensation |
|---|---|
| +3 | Hot |
| +2 | Warm |
| +1 | Slightly warm |
| 0 | Neutral |
| -1 | Slightly cool |
| -2 | Cool |
| -3 | Cold |

The thermal sensation scale for the air in cabin and the supplied air by AHU can be described respectively as follows:

$$\begin{aligned} dY_{IN}/dt = {} & \beta_\theta\{(\tilde{f}_c + \tilde{f}_h)(\theta_S - \theta_{IN})/V_{IN} + h_g\Omega_p(\tilde{f}_c + \tilde{f}_h)[(Y_S - \beta_\theta\theta_S - \beta_c) \\ & - (Y_{IN} - \beta_\theta\theta_{IN} - \beta_c)]/\beta_p c_p V_{IN} \\ & + A_W^{IN}\{\hat{h}_n + \hat{h}_f[(\tilde{f}_c + \tilde{f}_h)/S_{IN}]^{2/3}\}(\theta_W - \theta_{IN})/\rho_a c_p V_{IN} \\ & + A_W^{SH} \times SHGF \times (SHGC/0.87)/\rho_a c_p V_{IN} + Q_{load}/\rho_a c_p V_{IN}\} \\ & + \beta_p\{(\tilde{f}_c + \tilde{f}_h)[(Y_S - \beta_\theta\theta_S - \beta_c) - (Y_{IN} - \beta_\theta\theta_{IN} - \beta_c)]/V_{IN}\beta_p \\ & + M_{load}/\rho_a V_{IN}\Omega_p\} \end{aligned} \quad (7)$$

$$\begin{aligned} dY_S/dt = {} & \beta_\theta\{\tilde{f}_{mix}[(\tilde{f}_c\theta_C + \tilde{f}_h\theta_H)/(\tilde{f}_c + \tilde{f}_h) - \theta_S]/V_{HF} \\ & + h_g\Omega_p\tilde{f}_{mix}[\tilde{f}_c p_C/(\tilde{f}_c + \tilde{f}_h) + \tilde{f}_h(Y_{IN} - \beta_\theta\theta_{IN} - \beta_c)/(\tilde{f}_c + \tilde{f}_h)\beta_p \\ & - (Y_S - \beta_\theta\theta_S - \beta_c)/\beta_p]/c_pV_{HF}\} \\ & + \beta_p\{\tilde{f}_{mix}[\tilde{f}_c p_C/(\tilde{f}_c + \tilde{f}_h) + \tilde{f}_h(Y_{IN} - \beta_\theta\theta_{IN} - \beta_c)/\beta_p(\tilde{f}_c + \tilde{f}_h) \\ & - (Y_S - \beta_\theta\theta_S - \beta_c)/\beta_p]/V_{HF} + M_{HF}/\rho_a V_{HF}\Omega_p\} \end{aligned} \quad (8)$$

To sum up, the thermodynamic model of cabin and AHU can be described by these seven state equations ( i.e., (1) to (6) and (8)).

### E. Linearization of System Model

Since the air conditioning system is assumed to operate in a long time frame but be controlled to remain at certain constant temperature and relative humidity, the state equations, (1) to (6) and (8), can be linearized by taking Taylor's Expansion around an operational point. For simplicity, the linearized system model around the operational point will be named as "nominal plant" hereafter. The eigenvalues of the nominal open-loop system are shown in Fig. 2. It is observed from Fig. 2 that the eigenvalues of the nominal open-loop system can be clustered into two groups: fast mode and slow mode. In other words, the HVAC system possesses two-time-scale property. Therefore, the HVAC is a type of singular perturbation system.

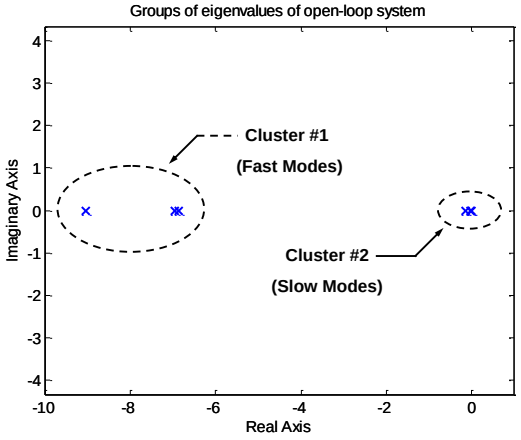


Fig. 2 Groups of Eigenvalues of Open-loop System

## III. MODEL REDUCTION BY SINGULAR PERTURBATION

The singular perturbation theory is often employed to deal with the plant with parasitic parameters. By singular perturbation approach, the original system model can be split into two reduced-order subsystems in two time scales, i.e., slow-mode subsystem and fast-mode subsystem.

In this paper, the ratio of volume of AHU with respect to that of cabin is defined as the singular perturbation parameter for the studied air-conditioning system. That is, the singular perturbation parameter, $\varepsilon$, is defined as:

$$\varepsilon = (V_{HT} + V_{HF})/V_{IN} \quad (9)$$

Assume the linearized plant model and the measurement can be expressed as follows [16]:

$$\begin{bmatrix} \dot{\mathbf{x}} \\ \varepsilon\dot{\mathbf{z}} \end{bmatrix} = \begin{bmatrix} \mathbf{A}_{11} & \mathbf{A}_{12} \\ \mathbf{A}_{21} & \mathbf{A}_{22} \end{bmatrix}\begin{bmatrix} \mathbf{x} \\ \mathbf{z} \end{bmatrix} + \begin{bmatrix} \mathbf{B}_1 \\ \mathbf{B}_2 \end{bmatrix}\mathbf{u}, \qquad \begin{bmatrix} \mathbf{x}(0) \\ \mathbf{z}(0) \end{bmatrix} = \begin{bmatrix} \mathbf{x}^0 \\ \mathbf{z}^0 \end{bmatrix} \quad (10)$$

$$\mathbf{y} = \begin{bmatrix} \mathbf{M}_1 & \mathbf{M}_2 \end{bmatrix}\begin{bmatrix} \mathbf{x} \\ \mathbf{z} \end{bmatrix} \quad (11)$$

where $\mathbf{x} \in \Re^n$, $\mathbf{z} \in \Re^m$, $\mathbf{u} \in \Re^r$ and $\mathbf{y} \in \Re^p$.

The original above (i.e. (10) and (11)) system can be

separated into two reduced-order subsystems:

(i) Slow-mode subsystem $(\mathbf{M}_0, \mathbf{A}_0, \mathbf{B}_0)$.

(ii) Fast-mode subsystem $(\mathbf{M}_2, \mathbf{A}_{22}, \mathbf{B}_2)$.

Hence, the state of the original system, $\tilde{\mathbf{x}}$, is divided into slow-mode state $\mathbf{x}$, and fast-mode state $\mathbf{z}$. For different seasons, these two state vectors can be defined as follows:

(i) Summer Mode:

$$\mathbf{x}_s = [\theta_{IN} \quad Y_{IN} \quad \theta_W]^{\mathrm{T}} \tag{12}$$

$$\mathbf{z}_s = [\theta_S \quad Y_S \quad \theta_H]^{\mathrm{T}} \tag{13}$$

(ii) Winter Mode:

$$\mathbf{x}_w = [\theta_{IN} \quad Y_{IN} \quad \theta_W]^{\mathrm{T}} \tag{14}$$

$$\mathbf{z}_w = [\theta_S \quad Y_S \quad \theta_H \quad \theta_{HT}]^{\mathrm{T}} \tag{15}$$

## IV. Near-optimal Reduced Controller Design

Since the system submatrix, $\mathbf{A}_{22}$, for either summer-mode or winter- mode is Hurwitz, the order-reduced controller can be synthesized by solely taking the slow-mode subsystem model into account. In other words, we can directly ignore the fast-mode stable subsystem to obtain the order-reduced controller. Hence, the near-optimal reduced controller can be constructed by simplifying as follows [16]:

$$\mathbf{u}_r = -\mathbf{R}_0^{-1}(\mathbf{N}_0^{\mathrm{T}}\mathbf{M}_0 + \mathbf{B}_0^{\mathrm{T}}\mathbf{K}_s)\mathbf{x} = -\mathbf{F}\begin{bmatrix}\mathbf{x}\\ \mathbf{z}\end{bmatrix} \tag{16}$$

where $\mathbf{F}$ is the feedback control gain.

## V. Computer Simulations

At the first stage, the proposed control policies: Near-optimal regulator, near-optimal reduced control and corrected Linear Quadratic Regulator (LQR) are examined by intensive computer simulations. In addition, the standard LQR plays the role of benchmark and is to be compared with the preliminarily proposed controllers by this work. The initial values and the desired values of the system outputs are summarized in Table II and Table III respectively.

TABLE II
INITIAL VALUES OF SYSTEM OUTPUT

| Preset Initial Values of System Output | | Value | |
|---|---|---|---|
| | | Summer | Winter |
| Temperature of air in cabin | $\theta_{IN}(0)$ | 30 °C | 16 °C |
| Thermal sensation scale of air in cabin | $Y_{IN}(0)$ | 1.5062 | –2.4197 |

TABLE III
DESIRED VALUES OF SYSTEM OUTPUT

| Set Values of System Output to Achieve | | Nominal Value | |
|---|---|---|---|
| | | Summer | Winter |
| Temperature of air in cabin | $\theta_{IN}^e$ | 25 °C | 22 °C |
| Thermal sensation scale of air in cabin | $Y_{IN}^e$ | 0 | 0 |

In addition, all the physical quantities of system parameters are listed in Table IV. Under various control strategies, the corresponding response of the system outputs, i.e., $\theta_{IN}$ and $Y_{IN}$, are shown in Fig. 3 to Fig. 6. It can be observed that the discrimination of the temperature response under various control policies is fairly limited. In other words, by splitting the original system model into two reduced-order subsystem models: slow mode and fast mode, the efficacy of various optimal controllers proposed by this paper is all acceptable, with respect to the benchmark by LQR. Furthermore, even if merely the slow-mode model, obtained by singular perturbation technique, is employed to replace the original system model, the degree of downgraded performance in terms of time response of the temperature and humidity regulation by the proposed control strategies is still satisfactory, to some extent. Since the near-optimal reduced controller is the simplest and carries least computation load, it is chosen for the efficacy verification of later-on experiments in the next section.

TABLE IV
SYSTEM PARAMETERS

| Parameter | | Value |
|---|---|---|
| Outdoor temperature (summer mode) | $\theta_{O,S}$ | 32 °C |
| Outdoor temperature (winter mode) | $\theta_{O,W}$ | 7 °C |
| Solar irradiation intensity (summer mode) | $I_{t,S}$ | 450 W/m$^2$ |
| Solar irradiation intensity (winter mode) | $I_{t,W}$ | 225 W/m$^2$ |
| Specific heat of air | $c_p$ | 1.005 kJ/kg ·°C |
| Density of air | $\rho_a$ | 1.225 kg/m$^3$ |
| Specific enthalpy of saturated vapor | $h_g$ | 2546.8 kJ/kg |
| Parameters of ASHRAE thermal sensation equation | $\beta_\theta$ | 0.245 °C$^{-1}$ |
| | $\beta_p$ | $0.248\times10^{-3}$ Pa$^{-1}$ |
| | $\beta_c$ | –6.475 |
| Natural convective heat transfer coefficient | $\hat{h}_n$ | 15 W/m$^2\cdot$K |
| Forced convective heat transfer coefficient | $\hat{h}_f$ | 160 W/m$^2\cdot$K |
| Heat capacity of cabin wall | $C_W$ | 4.908 kJ/ °C |
| Volume of air in cabin | $V_{IN}$ | 0.245 °C$^{-1}$ |
| Exterior surface area of cabin wall | $A_W^O$ | 0.451 m$^2$ |
| Interior surface area of cabin wall | $A_W^{IN}$ | 0.430 m$^2$ |
| Exterior irradiated surface area of cabin wall | $A_W^{SH}$ | 0.1 m$^2$ |
| Absorptance of solar radiation | $\alpha$ | 6% |
| Solar-Heat Gain Coefficient | $SHGC$ | 0.87 |

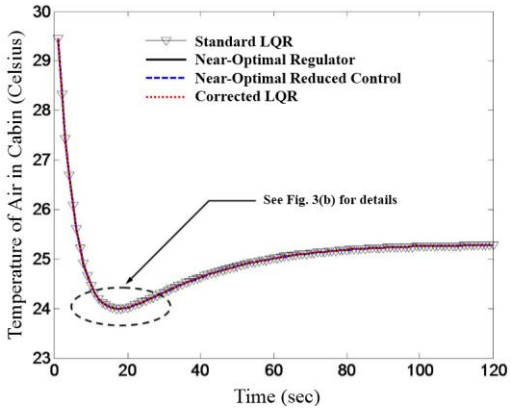


Fig. 3(a) Temperature of Air in cabin, $\theta_{IN}$ , at Summer Mode

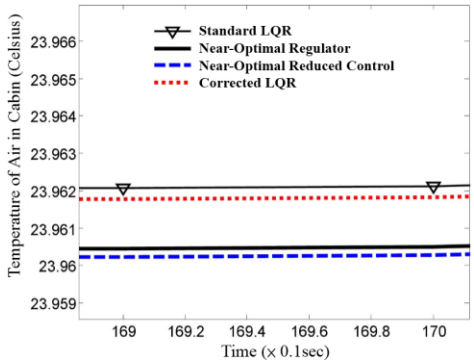


Fig. 3(b) Zoom-up of Lowest of Temperature of Air in Cabin, $\theta_{IN}$ , at Summer Mode

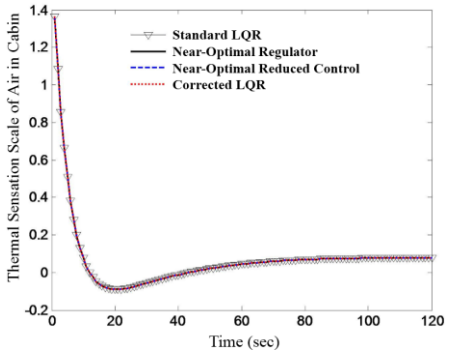


Fig. 4 Thermal Sensation Scale of Air in Cabin, $Y_{IN}$ , at Summer Mode

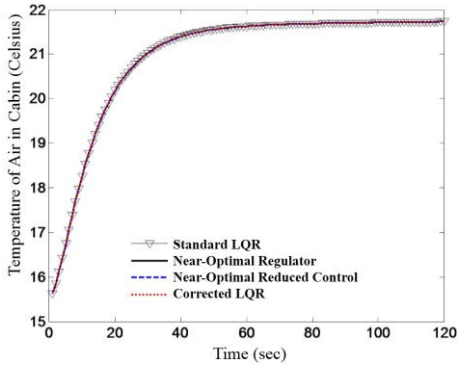


Fig. 5 Temperature of Air in Cabin, $\theta_{IN}$ , at Winter Mode

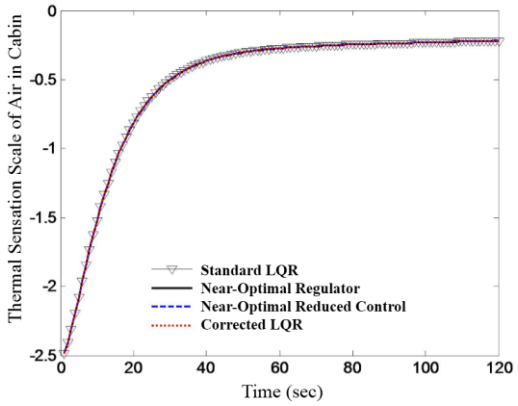


Fig. 6 Thermal Sensation Scale of Air in Cabin, $Y_{IN}$ , at Winter Mode

## VI. Experimental Results

In order to verify the efficacy of the proposed near-optimal reduced control strategy, intensive realistic experiments for HVAC are undertaken. The schematic diagram and its photography of the test rig are shown in Fig. 7 and Fig. 8 respectively. In the experimental test rig, by using the ECB (Environmental Control Box) to imitate the vehicle cabin, the interface module *DS1104* by *dSPACE* and the commercial software *MATLAB/Simulink* are employed to realize the proposed control loops. The interface module *DS1104* acquires the voltage signals in terms of the temperature in ECB, $\theta_{IN}$ , by the temperature sensor and the relative humidity in the ECB, $\phi_{IN}$ , by the humidity sensor respectively. In fact, the ASHRAE thermal sensation scale, $Y_{IN}$ , which is nothing but one of the system outputs, is the linear combination of $\theta_{IN}$ and the partial pressure of water vaporization, $p_v$ . The partial pressure of water vaporization, $p_v$ , can be obtained as follows [21]:

$$p_v = p_g \phi_{IN} \tag{17}$$

where $p_g$ is the saturated vapor pressure.

$$\ln(p_g) = 31.9602 - \frac{6270.3605}{\theta_{IN}} - 0.46057 \ln(\theta_{IN})$$

$$255.38\,\mathrm{K} \le \theta_{IN} \le 273.16\,\mathrm{K} \tag{18}$$

and

$$\ln\left(\frac{p_g}{R_c}\right) = \frac{A_c + B_c\theta_{IN} + C_c\theta_{IN}^{\ 2} + D_c\theta_{IN}^{\ 3} + E_c\theta_{IN}^{\ 4}}{F_c\theta_{IN} - G_c\theta_{IN}^{\ 2}}$$

$$273.16\,\mathrm{K} \le \theta_{IN} \le 533.16\,\mathrm{K} \tag{19}$$

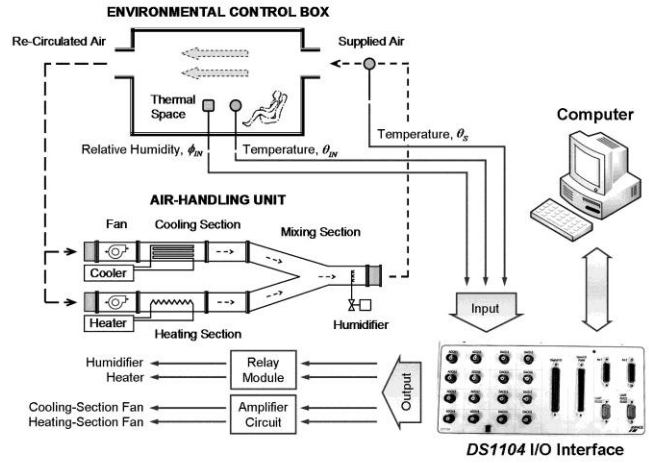


Fig. 7 Schematic Diagram of Experimental Test Rig

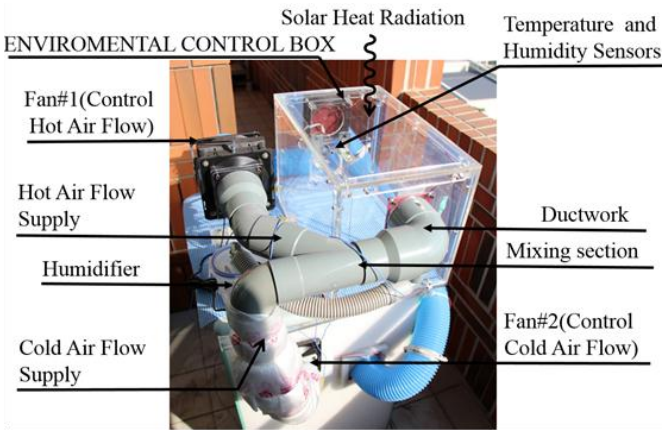


Fig. 8 Photography of Partial Experimental Test Rig (Outdoors)

By added-on power amplifier circuit modules to drive AHU, humidifier and electric heater, the performance of the proposed control law: near-optimal reduced control strategy, is examined. The desired system outputs under summer mode and winter mode of the ECB are preset in Table V and Table VI respectively.

TABLE V
DESIRED VALUES OF OUTPUT UNDER SUMMER MODE

| The Variables to be Preset | Summer Mode |
|---|---|
| Desired temperature of air in ECB () $\theta_{IN}^{e}$ | 25 ˚C |
| Desired thermal sensation scale of air in ECB environment ( $Y_{IN}^{e}$ ) | 0 (Neutral) |

TABLE VI
DESIRED VALUES OF OUTPUT UNDER WINTER MODE

| The Variables to be Preset | Winter Mode |
|---|---|
| Desired temperature of air in ECB ( $\theta_{IN}^{e}$ ) | 42 ˚C |
| Desired thermal sensation scale of air in ECB ( $Y_{IN}^{e}$ ) ( 42 ˚C , 50% RH ) | 4.8316 |

At summer mode, the local temperature of the atmospheric temperature is about $28 \sim 30$ ˚C. At winter mode, due to the subtropical environment of Taiwan, it is not cold at all. More importantly, in order to accomplish the experiments both for Summer Mode and Winter Mode during the same week, we always preset the ambient temperature as $28 \sim 30$ ˚C. However, to imitate Winter Mode, the desired temperature of the air in ECB is set as 42 ˚C so that it makes sense for the heating subsystem, instead of cooling subsystem, to the engaged. In the same manner, the corresponding ASHRAE thermal sensation scale for Winter Mode is referred to the relative humidity 50% and the temperature 42 ˚C.

The experimental results are shown in Fig. 9 to Fig.12. At summer mode, under near-optimal reduced control strategy, the AHU is able to regulate the temperature in the ECB to 25 ˚C, and limit the temperature fluctuation in the range of $\pm 0.5$ ˚C, as shown in Fig. 9. In comparison, once the control loop is removed, the temperature in ECB, shown in Fig. 9, will be continuously increased. After a certain period of time, the temperature of air in ECB, $\theta_{IN}$, is expected to be far higher than the atmosphere temperature since the solar energy is continuously absorbed by the ECB. The ASHRAE thermal sensation scale inside the ECB can be controlled to merely vary below $\pm 0.5$, i.e., the thermal comfortableness zone, and maintain at thermoneutral level ($Y = 0$), shown in Fig. 10. On the contrary, at winter mode, the AHU can heat the air in the ECB to the desired temperature 42 ˚C, shown in Fig. 11. The real-time actual ASHRAE thermal sensation scale, shown in Fig. 12, gradually merges to the desired value specified in Table VI.

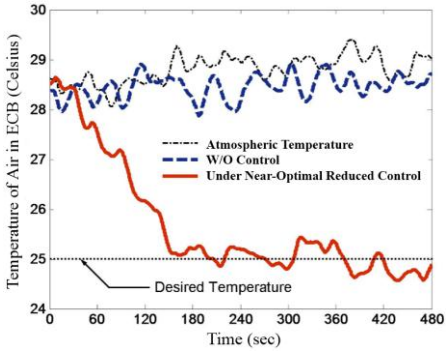


Fig. 9 Temperature of Air in ECB, $\theta_{IN}$, at Summer Mode

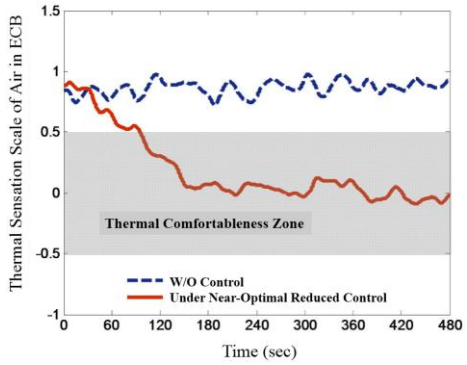


Fig. 10 Thermal Sensation Scale of Air in ECB, $Y_{IN}$ , at Summer Mode

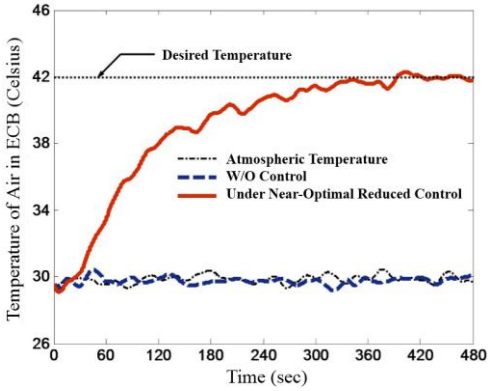


Fig. 11 Temperature of Air in ECB, $\theta_{IN}$ , at Winter Mode

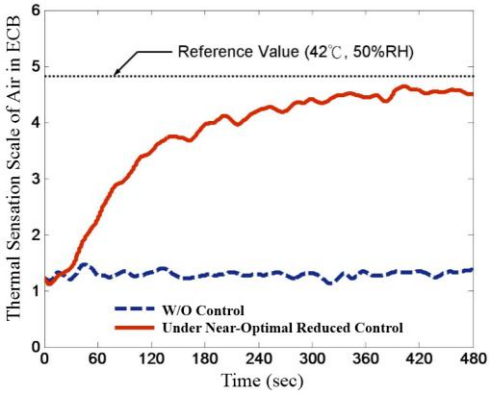


Fig. 12 Thermal Sensation Scale of Air in ECB, $Y_{IN}$ , at Winter Mode

## VII. Conclusion

In this study, a scale-down test rig of Heating, Ventilation, and Air Conditioning (HVAC), which mainly consists of the Environmental Control Box (ECB) and the Air-Handling Unit (AHU) to imitate the environment of cabin in vehicle, is constructed. The AHU module is constituted by the air cooling/heating sections, the mixing section and the humidifying section. The thermodynamic models of ECB and AHU are successfully derived and can be described by seven state equations. By system model linearization and singular perturbation technique, the studied system can be decoupled into two order-reduced subsystems: slow-mode subsystem and fast-mode subsystem. A series of optimal controllers, namely near-optimal regulator, near-optimal reduced control and corrected linear quadratic regulator, are proposed for the studied HVAC system. According to the computer simulation results, the efficacy of various optimal controllers developed by our work is all acceptable, with respect to the benchmark by LQR. The near-optimal reduced control strategy is the simplest and carries the least computation load so that it is chosen for the follow-up efficacy examination by experiments. The experimental results show that under near-optimal reduced control law, AHU is able to regulate the temperature in the ECB to 25 ˚C , and continue to stay thermoneutral at summer mode. On the other hand, at winter mode, the AHU is able to heat the air in the ECB up to the preset temperature. In addition, the time response of actual ASHRAE thermal sensation scale gradually tends to achieve the desired value. By experiments, it is preliminarily verified that the near-optimal reduced control strategy is almost as superior as that by Linear Quadratic Regulator (LQR).

## Acknowledgment

This research was partially supported by National Science Council (Taiwan) with Grant 102-2221-E-006-229-MY3, and the authors would like to express their appreciation.

## References

[1] J. Erjavec, J. Arias, “Hybrid, electric and fuel-cell vehicles,” Thomson Delmar Learning, Australia, 2007.
[2] B. Tashtoush, M. Molhim, M. Al-Rousan, “Dynamic model of an HVAC system for control analysis” Energy, Vol. 30, No. 10, pp. 1729-1745, 2005
[3] M. R. Kulkarni, F. Hong, “Energy optimal control of a residential space-conditioning system based on sensible heat transfer modeling,” Building and Environment, Vol. 39, No. 1, pp. 31-38, 2004.
[4] O. Arici, S.-L. Yang, D. Huang, E. Oker, “Computer model for automobile climate control system simulation and application,” International Journal of Applied Thermodynamics, Vol. 2, No. 2, pp. 59-68, 1999.
[5] G. Platt, J. Li, R. Li, G. Poulton, G. James, J. Wall, “Adaptive HVAC zone modeling for sustainable buildings,” Energy and Buildings, Vol. 42, No. 4, pp. 412-421, 2010.
[6] J. Li, G. Poulton, G. Platt, J. Wall, G. James, “Dynamic zone modelling for HVAC system control,” International Journal of Modelling, Identification and Control, Vol. 9, No. 1-2, pp. 5-14, 2010.
[7] T. Tabe, K. Matsui, T. Kakehi, M. Ohba, “Automotive climate control,” IEEE Control Systems Magazine, Vol. 6, No. 5, pp. 20-24, 1986.
[8] C. Ghiaus, A. Chicinas, C. Inard, “Grey-box identification of air-handling unit elements,” Control Engineering Practice, Vol. 15, No. 4, pp. 421-433, 2007.
[9] G. R. Zheng, M. Zaheer-Uddin, “Optimization of thermal processes in a variable air volume HVAC system,” Energy, Vol. 21, No. 5, pp. 407-420, 1996.
[10] S. Wang, X. Jin, “Model-based optimal control of VAV air-conditioning system using genetic algorithm,” Building and Environment, Vol. 35, No. 6, pp. 471-487, 2000.
[11] S. Atthajariyakul, T. Leephakpreeda, “Real-time determination of optimal indoor-air condition for thermal comfort, air quality and efficient energy usage,” Energy and Buildings, Vol. 36, No. 7, pp. 720-733, 2004.
[12] X. Xu, S. Wang, Z. Sun, F. Xiao, “A model-based optimal ventilation control strategy of multi-zone VAV air-conditioning systems,” Applied Thermal Engineering, Vol. 29, No. 1, pp. 91-104, 2009.
[13] M. Mossolly, K. Ghali, N. Ghaddar, “Optimal control strategy for a multi-zone air conditioning system using a genetic algorithm,” Energy, Vol. 34, No. 1, pp. 58-66, 2009.

[14] M. A. Salman, A. Y. Lee, N. M. Boustany, "Reduced order design of active suspension control," Trans. on ASME J. Dynamic Systems, Measurement, and Control, Vol. 112, No. 4, pp. 604-610, 1990.
[15] A. Hac, "Decentralized control of active vehicle suspensions with preview," Trans. on ASME J. Dynamic Systems, Measurement, and Control, Vol. 117, No. 4, pp. 478-483, 1995.
[16] P. V. Kokotovic, H. K. Khalil, J. O'Reilly, "Singular Perturbation Methods in Control: Analysis and Design," Academic Press, London, 1986.
[17] C. C. Federspiel, "User-Adaptable and Minimum-Power Thermal Comfort Control," PhD dissertation, Dept. Mech. Eng., Massachusetts Institute of Technology, Cambridge, MA, 1992.
[18] F. Kreith, W. Z. Black, "Basic Heat Transfer," Harper & Roll, New York, 1980.
[19] ANSI/ASHRAE Standard 55-1992, "Thermal Environmental Conditions for Human Occupancy," American Society of Heating, Refrigerating, and Air-Conditioning Engineers, Inc., Atlanta, GA, 1992.
[20] "ASHRAE handbook: Fundamentals Volume," American Society of Heating, Refrigerating, and Air-Conditioning Engineers, Inc., Atlanta, GA, 1997.
[21] "ASAE Standards: Standards, Engineering Practices and Data 45th ed.," American Society of Agricultural Engineers, St. Joseph, MI, 1998.